

## Article

# Different Land-Use Effects on Soil Aggregates and Aggregate-Associated Organic Carbon in Eastern Qinghai–Tibet Plateau

Yongkun Zhang <sup>1</sup>, Ying Li <sup>1</sup>, Zhanming Ma <sup>1</sup>, Zilong Cui <sup>1</sup>, Haiyan Sheng <sup>2</sup> and Runjie Li <sup>1,\*</sup>

<sup>1</sup> State Key Laboratory of Plateau Ecology and Agriculture, Qinghai University, Xining 810016, China; zhangyongkun321@163.com (Y.Z.); 15175791731@163.com (Y.L.); 15110925674@163.com (Z.M.); cuizilong130182@163.com (Z.C.)

<sup>2</sup> College of Agriculture and Animal Husbandry, Qinghai University, Xining 810016, China; xnshy26@sina.com

\* Correspondence: rjl@126.com

**Abstract:** Land use changes modify soil properties, including aggregate structure, and thus, profoundly affect soil quality and health. However, the effects of land use changes originating from alpine grassland on soil aggregates and aggregate-associated organic carbon have received little attention. Soil aggregate fraction, aggregate-associated organic carbon and relevant influencing factors were determined at 0–20, 20–40 cm soil layers for alpine grassland, cropland and abandoned land in the eastern Qinghai–Tibet Plateau (QTP), and their relationships were analyzed by partial least square regression (PLSR). Results showed the following: (1) conversion from alpine grassland to cropland resulted in a significant decline macroaggregate fraction ( $R_{0.25}$ ), mean weight diameter (MWD), mean weight diameter (GMD), soil organic carbon (SOC), and microaggregate-associated SOC; (2) almost all aggregate stability indexes, SOC, and aggregate-associated SOC were significantly positively correlated with silt and glomalin, suggesting that the binding of fine particles (silt) with the organic cementing agent (glomalin) was probably a key mechanism of SOC formation and aggregate stability in the studied region; (3) compared with biotic factors such as SOC, glomalin and root biomass, abiotic factors including silt and sand can better predict aggregate stability and SOC fraction using the PLSR model. The above results indicated that the conversion of alpine grassland to other land use types in high altitude areas would destroy soil structure and decrease soil organic carbon content, and then reduce soil quality.

**Keywords:** soil aggregate stability; soil quality; LUCC; alpine grassland



**Citation:** Zhang, Y.; Li, Y.; Ma, Z.; Cui, Z.; Sheng, H.; Li, R. Different Land-Use Effects on Soil Aggregates and Aggregate-Associated Organic Carbon in Eastern Qinghai–Tibet Plateau. *Agronomy* **2024**, *14*, 990. <https://doi.org/10.3390/agronomy14050990>

Academic Editor: Yash Dang

Received: 26 February 2024

Revised: 26 April 2024

Accepted: 29 April 2024

Published: 8 May 2024



**Copyright:** © 2024 by the authors. Licensee MDPI, Basel, Switzerland. This article is an open access article distributed under the terms and conditions of the Creative Commons Attribution (CC BY) license (<https://creativecommons.org/licenses/by/4.0/>).

## 1. Introduction

Soil fertility and land degradation are affectable due to SOC relations with soil structure, nutrient retention, water storage and pollutant attenuation [1]. Soil aggregate is the most fundamental soil structural unit [2]. Good aggregate structure can help the soil retain better water, fertilizer, gas and heat conditions, and thus, obtain better soil quality [3]. SOC tends to be regarded as one of the key indicators of soil quality [4]. As the concentrated embodiment of soil organic-cementing material, SOC is conducive to promoting the formation of soil macroaggregates and improving soil structure [5]. Contrary to this, soil aggregates can not only physically protect SOC from microbial decomposition, but also adsorb SOC on the surface of clay particles through chemisorption, thus reducing SOC loss [6,7]. Therefore, exploring the properties of soil aggregates and SOC and their relationships is of great significance for evaluating soil quality [8].

Land use/land cover change (LUCC) is the primary human activity driving soil structure and organic carbon storage change [9–12]. Due to low temperatures, drought and weak microbial activity from high altitude, the decomposition, stability and accumulation of SOC in alpine grassland are different from those in the grasslands of other climate

types [13,14]. Regional differences of SOC further trigger the particularity of the soil aggregate structure in alpine grassland [15]. Therefore, it is necessary to explore the effects of LUCC originating from alpine grassland on SOC and aggregate structure.

Previous studies regarding the effects of land use/land cover change originating from alpine grassland on SOC and aggregate structure mainly focused on grassland degradation triggered by overgrazing [13,16,17] (that is, the role of land cover change), less concerned with land use change [18] (such as the conversion of grassland to cropland). Ma et al. (2020) found that, with the degradation of an alpine meadow, the soil macroaggregate percentage decreased, MWD and GMD became smaller, and SOC within microaggregate was higher than that of other aggregate fractions [16]. Dong et al. (2020) compared and analyzed the non-degraded and degraded grasslands of an alpine meadow and alpine steppe, and reported that the microaggregate-associated SOC of a non-degraded alpine meadow was highest among all grassland types; the macroaggregate-associated SOC of degraded grassland was higher than that of a non-degraded grassland [13]. Pu et al. (2022) suggested that with the degradation of alpine marsh meadows, soil macroaggregates and SOC decreased significantly; aliphatic C decreased, and alcohol phenolic C and polysaccharide C increased in SOC fractions as the alpine marsh meadow degraded [17]. Land use significantly affected soil properties and quality [9]. The land use conversion of grassland, cropland and abandoned land, as one of the main forms of land use conversion, had profound impacts on soil aggregates and SOC and had been widely concerned worldwide [9,19–21]. Studies on soil aggregates, SOC and their relationships during land use conversion from alpine grassland to cropland and abandoned land are rather rare, and the varying mechanism is still unclear.

Due to low temperatures, weak microbial activity and long-time accumulation, the composition and storage of SOC and soil aggregate structure in alpine grassland differ remarkably from those in a low-altitude area [11–13]. Despite substantial studies on the effects of land use change on soil aggregates and SOC with aggregate fractions, few studies are focused on the contribution of land use change starting from alpine grassland to soil aggregates and aggregate-associated SOC, and the influencing mechanism is still unclear. In the study, soil aggregate fraction, stability, SOC, aggregate-associated SOC and corresponding influencing factors (pH, soil particle, root biomass, etc.) were measured and calculated at 60 sampling sites in the eastern QTP. Based on the above measurements, we aimed to test the hypothesis that soil aggregate and aggregate-associated SOC varied significantly with the conversion of alpine grassland into crop and abandoned land, and abiotic factors had more influence on such changes than biotic factors. Therefore, the objectives of this study were as follows: (1) to evaluate the response of soil aggregate fractions, stability and aggregate-associated SOC to land use change originating from alpine grassland; and (2) to identify key controls driving soil aggregate stability and aggregate-associated SOC during land use conversion in alpine grassland.

## 2. Materials and Methods

### 2.1. Sites

The study area is located in Minhe, Pingan, Huzhu, Huangzhong, and Ledu County, Qinghai Province (101°41′–103°42′ E, 36°06′–37°08′ N) in the eastern part of the Qinghai–Tibet Plateau (Figure 1). The conversions of grassland, cropland and abandoned land in this region are most drastic in the Qinghai–Tibet Plateau [22]. With the social and economic development in the region, large numbers of grasslands had been reclaimed for cropland. Due to the policy of “Grain for Green Project”, part of the cropland in the region was abandoned [23,24]. The terrain is mainly hilly, with elevations between 1767 and 2275 m. It is a plateau continental climate, with an annual mean temperature between 3.1–7.9 °C (1960–2017) and annual mean precipitation at 381.1 mm (1960–2017) [25]. The soil type in this area is mainly chestnut soil. The area has been cultivated for nearly 300 years [24], mainly implementing a rotation system of one crop a year. The final crops on the collected soil are spring wheat (*Triticum aestivum* L.), spring corn (*Zea mays* L.), potato (*Solanum*

*tuberosum* L.), and spring rape (*Brassica campestris* L.), which are also the dominant crop in the region.

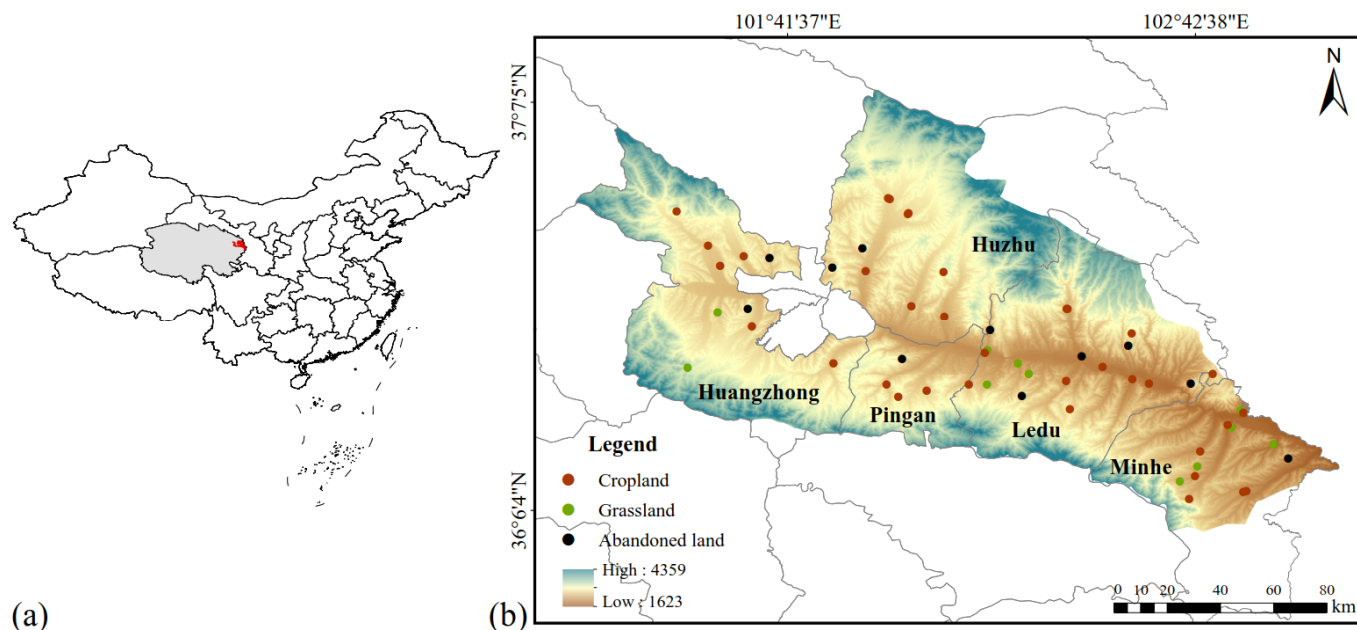


**Figure 1.** The study area location (a) and sampling site distribution in the studied area (b).

## 2.2. Samplings and Measurements

### 2.2.1. Experimental Design and Sampling

In September 2020 and April 2021, three land use types (grassland, cropland and abandoned land) were selected in Minhe, Ledu, Huzhu, Pingan, and Huangzhong County in eastern Qinghai Province to set up sampling sites. Eventually, a total of 60 sampling sites were selected, which were 11 samples in grassland, 38 samples in cropland and 11 samples in abandoned land. A root drill (inner diameter 9 cm) was used to collect a total of 120 soil samples from 0–20 and 20–40 cm soil layers at each sampling site. Each sampling site was set up with 5 replicates, and the soil sample with 5 replicates was removed from large impurities and fully mixed into one sample for the determination of soil aggregate fractions and SOC. Land use types were investigated before soil samples were collected and field management surveys were conducted through interviews with local farmers. After natural air drying in the room, the soil samples were put into the numbered plastic bags, sealed and stored for use.

### 2.2.2. Aggregate Separation and Soil Properties

Soil aggregate fraction, particle composition, organic carbon, pH, root dry weight, easily extractable glomalin-related soil protein (EE-GRSP) and total glomalin-related soil protein (T-GRSP) were determined and presented in Table 1. In this study, soil aggregates were determined by the wet sieve method, and the aggregates were sieved into fractions of >0.25 mm (macroaggregate), 0.25–0.053 mm (microaggregate) and <0.053 mm (silt + clay) [26]. The soil particle composition was determined by Mastersizer 3000 laser particle size analyzer (Malvern Instruments, Malvern, UK). The soil particle composition consisted of clay (<2  $\mu\text{m}$ ), silt (50–2  $\mu\text{m}$ ) and sand (2000–50  $\mu\text{m}$ ). The SOC content was analyzed using the dichromate oxidation method; about 0.60 g of air-dried soil was digested with 5 mL of 0.8 M  $\text{K}_2\text{Cr}_2\text{O}_7$  and 5 mL of  $\text{H}_2\text{SO}_4$  at 170–180  $^\circ\text{C}$  for 5 min, and the digestate was then titrated with 0.2 M  $\text{FeSO}_4$  [27]. Soil pH was measured in a 1:2.5 (air-dried soil–water) suspension using a pH meter with a glass electrode; the dry weight of soil roots was determined by the weighing method, that is, the roots (>1 mm) were washed out by a sieve with a diameter of 1 mm, dried in an oven at 65  $^\circ\text{C}$  and weighed. Glomalin-related

soil protein (GRSP) was determined based on the Bradford protein assay [28], which could be classified into two GRSP fractions including easily extractable glomalin-related soil protein (EE-GRSP) and total glomalin-related soil protein (T-GRSP).

**Table 1.** Basic information of different land use types.

Properties	Grassland		Cropland		Abandoned Land	
	0–20 cm	20–40 cm	0–20 cm	20–40 cm	0–20 cm	20–40 cm
pH	8.16 ± 0.07 a	8.2 ± 0.43 A	8.15 ± 0.18 a	8.34 ± 0.22 A	8.22 ± 0.11 a	7.72 ± 2.1 A
RDWD (g m <sup>-3</sup> )	1.47 ± 0.80 a	0.98 ± 0.68 A	0.53 ± 0.36 b	0.23 ± 0.26 B	0.54 ± 0.34 b	0.13 ± 0.07 B
SOC (g kg <sup>-1</sup> )	20.21 ± 4.22 a	15.03 ± 3.17 A	14.51 ± 5.28 b	11.00 ± 5.15 B	10.12 ± 6.62 c	10.13 ± 5.58 B
D <sub>50</sub> (μm)	1.84 ± 7.61 a	17.45 ± 3.24 A	21.83 ± 7.61 a	19.29 ± 6.97 A	20.86 ± 6.70 a	21.71 ± 7.74 A
Clay (%)	8.57 ± 1.63 a	8.52 ± 1.55 A	8.22 ± 1.54 a	9.59 ± 2.84 A	8.65 ± 3.32 a	8.88 ± 5.13 A
Silt (%)	73.85 ± 6.26 a	72.53 ± 3.58 A	70.55 ± 6.54 a	71.99 ± 5.77 A	72.61 ± 6.02 a	70.50 ± 4.29 A
Sand (%)	16.51 ± 4.66 a	18.03 ± 3.56 A	21.23 ± 7.89 a	18.41 ± 7.23 A	18.73 ± 7.77 a	20.24 ± 7.66 A
D <sub>v</sub> (mm)	2.72 ± 0.02 a	2.71 ± 0.02 A	2.71 ± 0.02 a	2.71 ± 0.03 A	2.72 ± 0.02 a	2.72 ± 0.02 A
T-GRSP (mg g <sup>-1</sup> )	2.89 ± 0.27 a	2.11 ± 0.36 A	2.43 ± 0.45 b	2.06 ± 0.52 A	2.38 ± 0.53 b	1.77 ± 0.64 A
EE-GRSP (mg g <sup>-1</sup> )	0.64 ± 0.13 a	0.47 ± 0.15 A	0.54 ± 0.13 a	0.46 ± 0.11 AB	0.54 ± 0.16 a	0.37 ± 0.12 C

Note: The values are the mean and standard deviation. Different capital and minuscule letters mean a remarkable difference in the same soil layer at different locations ( $p < 0.05$ ). RDWD indicates root dry weight density; SOC indicates soil organic carbon content; EE-GRSP indicates easily extractable glomalin-related soil protein; T-GRSP indicates total glomalin-related soil protein; and D<sub>v</sub> indicates volume-based fractal dimension.

### 2.3. Statistical Analysis

Aggregate stability is represented by mean weight diameter (MWD), mean geometric diameter (GMD), fractal dimension ( $D$ ) and macroaggregate fraction with diameter  $> 0.25$  mm ( $R_{0.25}$ ), and the corresponding formula is as follows:

$$MWD = \sum_{i=1}^n x_i \times w_i \quad (1)$$

$$GMD = \exp \left[ \frac{\sum_{i=1}^n w_i \times \ln x_i}{\sum_{i=1}^n w_i} \right] \quad (2)$$

where  $x_i$  is the mean diameter of the aggregate class (mm), and  $w_i$  is the proportion of each aggregate class in relation to the aggregate weights as follows:

$$\left[ \frac{\bar{d}_i}{d_{max}} \right]^{3-D} = \frac{W(r < \bar{x}_i)}{W_0} \quad (3)$$

where  $D$  is the fractal dimension,  $\bar{d}_i$  is the mean aggregate diameter (mm) of the  $i$  size class,  $d_{max}$  is the mean diameter of the largest aggregate,  $W(r < \bar{x}_i)$  is the cumulative mass of the aggregates of  $i$  size less than  $d_{max}$ , and  $W_0$  is the total mass of the aggregates.

Partial least squares regression model (PLSR) is a method suitable for analyzing multiple regressions with high autocorrelation, which is a combination of linear regression, canonical correlation and principal component analysis [29]. For this method, check whether the data conform to the normal distribution, and make the data conform to the normal distribution by logarithmic transformation. Then, data were imported into SIMCA 14.1 (Umetrics AB, Umea, Sweden) to determine the number of the components of independent variables using cross-validation, and the final number of components was determined according to the variance ratio of dependent variables. Eventually, the explanatory ability of independent variables in relation to dependent variables was evaluated by the variable projection importance (VIP) value. In general, a predictor variable with a VIP value higher than 1 has significant explanatory significance for the response variable, a medium level of interpretability when the VIP value is between 0.8 to 1, and no interpretation if the VIP value is lower than 0.8 [29,30]. The independent variables in this study have serious

correlation, and partial least squares regression can be used for regression modeling under this condition.

A one-way ANOVA with an LSD test was used to analyze the significance of soil properties, aggregate fractions, and aggregate-associated SOC across different land use types. Additionally, a two-way ANOVA was conducted to examine the effects of land use, soil depth, and their interaction on soil properties, aggregate stability, and aggregate-associated SOC. Excel, SPSS 25.2, and Origin 2021 were used for all statistical analyses.

### 3. Results

#### 3.1. Soil Aggregate Fraction and Stability

The distribution of aggregate size fractions under different land uses was summarized in Table 2. In 0–20 and 20–40 cm soil layers, with the conversion of grassland into cropland, the proportion of macroaggregate (>0.25 mm), MWD and GMD decreased significantly; the proportion of microaggregate (0.053–0.25 mm), the proportion of silt + clay fraction (<0.053 mm) and D significantly increased (Table 2, Figure 2). This indicated that land use change could affect soil aggregate structure remarkably, which was also supported by the results in Table 3.

**Table 2.** Distribution of aggregate size fractions (%) under different land uses.

Land Use	Soil Aggregate Fraction		
	>0.25 mm	0.053–0.25 mm	<0.053 mm
0–20 cm			
Grassland	63.06 ± 11.24 a <sup>1</sup>	27.32 ± 8.26 b	9.63 ± 3.60 b
Cropland	35.88 ± 18.86 b	46.43 ± 15.19 a	17.69 ± 5.17 a
Abandoned land	39.09 ± 16.60 b	44.07 ± 14.75 a	16.85 ± 4.77 a
20–40 cm			
Grassland	60.82 ± 5.93 a	28.91 ± 3.33 b	10.27 ± 4.26 b
Cropland	28.27 ± 19.11 b	50.53 ± 15.89 a	21.20 ± 6.91 a
Abandoned land	40.37 ± 18.71 b	42.26 ± 12.75 a	17.10 ± 8.15 a

Note: <sup>1</sup> different lower-case letters in a row mean significant differences ( $p < 0.05$ ).

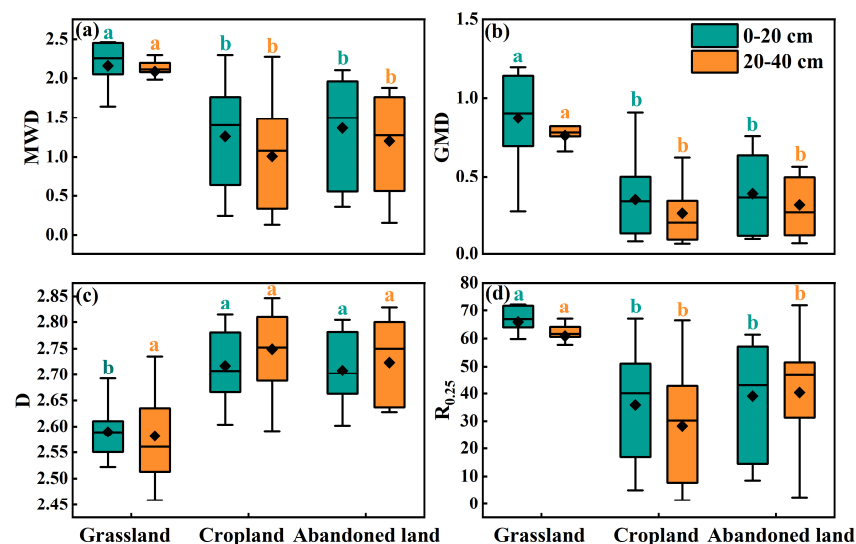


**Figure 2.** Changes in soil aggregate stability at 0–20 cm and 20–40 cm depths with land use types. Note: MWD indicates mean weight diameter (a); GMD indicates mean geometric diameter (b); D indicates fractal dimension (c);  $R_{0.25}$  indicates macroaggregate fraction with diameter > 0.25 mm (d).

**Table 3.** Analysis of variance results for the composition and stability of soil aggregates.

Soil Aggregate	Land Use		Soil Depth		Land Use × Soil Depth	
	F	<i>p</i>	F	<i>p</i>	F	<i>p</i>
Soil aggregate stability						
R <sub>0.25</sub>	16.230	<0.001	0.370	0.257	0.278	0.758
D	16.341	<0.001	1.298	0.054	0.015	0.985
MWD	35.649	<0.001	3.807	0.679	0.590	0.556
GMD	31.004	<0.001	0.173	0.545	0.784	0.460
Soil aggregate fraction						
Macroaggregate	16.230	<0.001	0.370	0.545	0.278	0.758
Microaggregate	11.643	<0.001	0.188	0.665	0.247	0.782
Silt + clay	17.305	<0.001	0.553	0.459	1.305	0.276

Note: MWD indicates mean weight diameter; GMD indicates mean geometric diameter; R<sub>0.25</sub> indicates macroaggregate fraction with diameter > 0.25 mm; D indicates fractal dimension.

After the cropland was converted to abandoned land, the proportion of macroaggregate (>0.25 mm), MWD, GMD and R<sub>0.25</sub> increased, but not significantly (Table 2, Figure 2,  $p > 0.05$ ), suggesting that abandonment in the studied area could improve soil structure to a limited extent. According to Tables 2 and 3, and Figure 2, no significant difference in aggregate fraction and stability between 0–20 and 20–40 cm soil layers was detected in grassland, cropland and abandoned land.

### 3.2. Soil Aggregate-Associated SOC

Bulk SOC was significantly reduced as grassland was successively transformed into cropland and abandoned land ( $p < 0.05$ , Table 4). Considering the SOC fraction, the SOC in each aggregate fraction decreased gradually following the conversion of grassland into cropland and abandoned land ( $p < 0.05$ , Table 4), suggesting that the reduction in aggregate-associated SOC during grassland succession contributed significantly to bulk SOC.

**Table 4.** Soil organic carbon content (g kg<sup>-1</sup>) in bulk soil and different aggregate fractions under various land use types.

Land Use	SOC <sup>1</sup>	Soil Aggregate Fraction		
		>0.25 mm	0.053–0.25 mm	<0.053 mm
0–20 cm				
Grassland	20.22 ± 4.23 a <sup>2</sup>	21.87 ± 4.45 a	16.66 ± 3.74 a	16.30 ± 5.46 a
Cropland	14.51 ± 5.29 b	19.26 ± 8.07 ab	11.96 ± 6.62 b	14.82 ± 7.58 ab
Abandoned land	10.00 ± 5.13 c	15.74 ± 6.14 b	10.30 ± 4.84 b	10.13 ± 6.62 b
20–40 cm				
Grassland	15.03 ± 3.17 a	15.96 ± 4.76 a	13.97 ± 5.35 a	12.89 ± 4.12 a
Cropland	11.00 ± 5.14 b	15.45 ± 7.75 a	9.04 ± 4.44 b	10.40 ± 5.96 a
Abandoned land	10.13 ± 5.58 b	10.64 ± 4.89 a	7.94 ± 3.82 b	9.56 ± 4.22 a

Note: <sup>1</sup> soil organic carbon; <sup>2</sup> different lower-case letters in a row mean significant differences ( $p < 0.05$ ).

According to Tables 4 and 5, bulk SOC decreased to a certain extent with the soil depth ( $p = 0.091$ ). From the perspective of the SOC fraction, the significant reduction in macroaggregate-associated SOC with soil depth ( $p < 0.05$ , Tables 4 and 5) resulted in decreasing bulk SOC. In contrast, SOC within the silt + clay fraction did not significantly decrease with soil depth ( $p = 0.205$ , Table 5).

**Table 5.** Effects of land use, soil depth and their interaction on soil aggregate-associated organic carbon.

SOC <sup>1</sup>	Land Use		Soil Depth		Land Use × Soil Depth	
	F	<i>p</i>	F	<i>p</i>	F	<i>p</i>
Bulk soil	8.624	<0.001	2.911	0.091	0.925	0.400
Macroaggregate	4.078	<0.05	8.080	<0.05	0.162	0.850
Microaggregate	8.829	<0.001	2.849	0.095	0.096	0.909
Silt + clay	2.948	<0.05	1.630	0.205	0.547	0.580

Note: <sup>1</sup> soil organic carbon.

### 3.3. Factors Controlling Soil Aggregates and Aggregate-Associated SOC

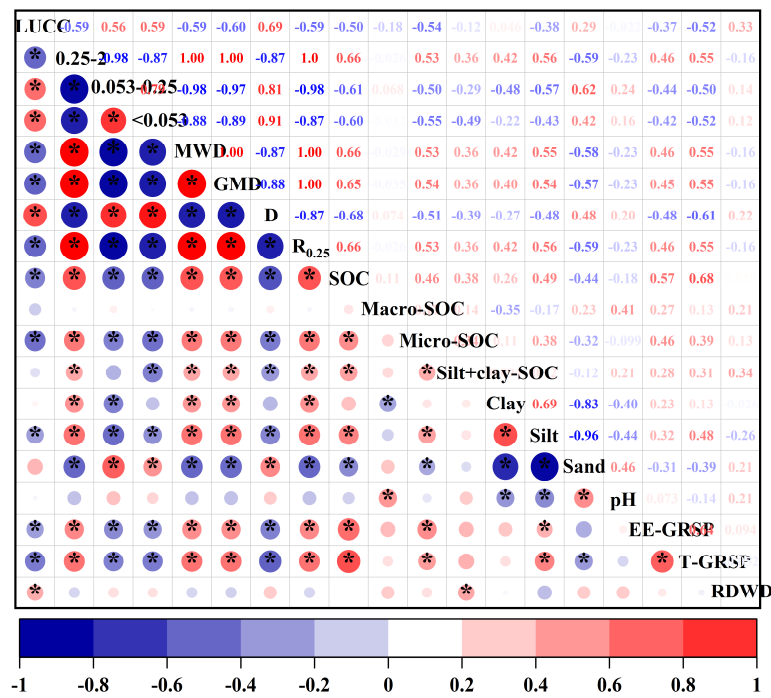
In the 0–20 soil layer, SOC within the silt + clay fraction was positively correlated with clay, silt and easily extractable and total glomalin-related soil protein (EE-GRSP, T-GRSP), and negatively correlated with the sand, but the correlation was not significant (Figure 2a,  $p > 0.05$ ). There was a significant positive correlation between microaggregate-associated SOC and silt, EE-GRSP, T-GRSP, and a significant negative correlation between microaggregate-associated SOC and sand (Figure 3a,  $p < 0.05$ ). In addition, significant positive correlation between microaggregate-associated SOC and silt + clay-associated SOC (Figure 3a,  $p < 0.05$ ) was observed. Macroaggregate-associated SOC was positively associated with the SOC within microaggregate (Figure 3a,  $p < 0.05$ ), but no significant interaction was detected between macroaggregate-associated SOC and soil particles, EE-GRSP, and T-GRSP (Figure 3a,  $p > 0.05$ ). SOC had significant positive correlation with microaggregate-associated SOC, silt + clay-associated SOC, silt content, EE-GRSP and T-GRSP (Figure 3a,  $p > 0.05$ ). In the 20–40 cm soil layer, relationships between SOC, SOC within aggregate fractions, and the influencing factors were typically the same as those in the 0–20 cm surface layer (Figure 3), except that the correlation between pH and multiple indexes was significantly enhanced (Figure 3b,  $p < 0.05$ ).

Through partial least squares regression (PLR) and variable projection importance (VIP) analysis, VIP scores of both silt and clay contents were higher than 1, exhibiting good prediction ability for SOC within aggregate fractions in 0–20 and 20–40 cm soil layers (Figure 4). Apart from silt and sand contents, SOC and root biomass in the 0–20 cm soil layer can be good predictors of SOC within the silt + clay fraction; clay content in the 20–40 cm soil layer can well estimate SOC in each aggregate fraction (Figure 4).

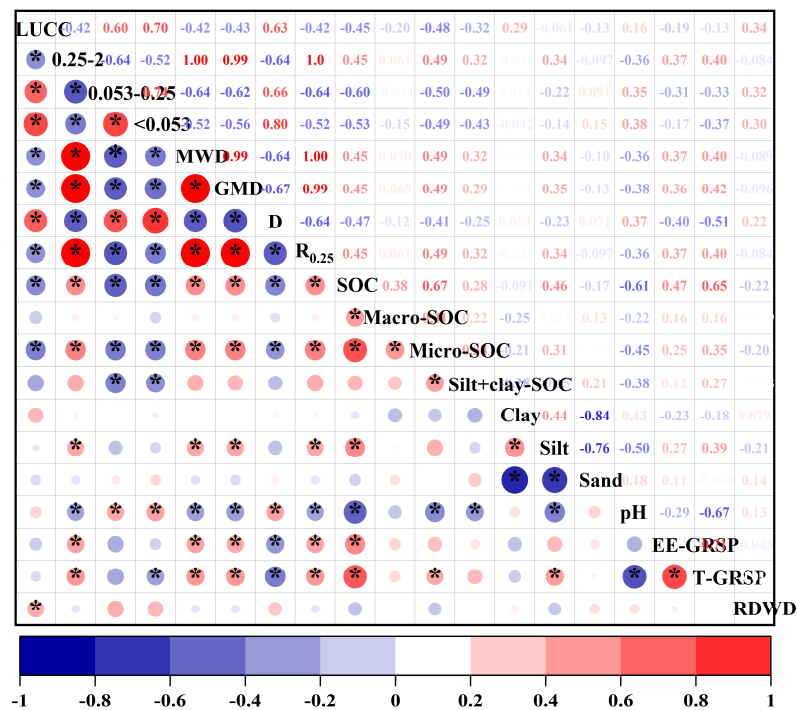
### 3.4. Factors Controlling Soil Aggregate Stability

In the 0–20 cm soil layer,  $R_{0.25}$ , MWD, and GMD, which represent aggregate stability, were significantly positively correlated with SOC, and the correlation coefficients were 0.66, 0.65, and 0.66, successively (Figure 3a,  $p < 0.01$ ). Further analysis from the perspective of SOC fractions showed that no remarkable associations between  $R_{0.25}$ , MWD, GMD and macroaggregate-associated SOC were identified (Figure 3a,  $p > 0.05$ ); significant positive correlations between soil aggregate stability indexes and SOC within microaggregate and silt + clay fraction were observed (Figure 3a,  $p < 0.05$ ). Considering soil particle composition, aggregate stability indexes ( $R_{0.25}$ , MWD, GMD) were significantly positively correlated with silt and clay content, and significantly negatively regulated by sand content (Figure 3a,  $p < 0.05$ ). Furthermore, significant positive correlations were detected between aggregate stability indexes ( $R_{0.25}$ , MWD, GMD) and EE-GRSP and T-GRSP (Figure 3a,  $p < 0.05$ ). In the 20–40 cm soil layer, relationships between soil aggregate stability indexes and the influencing factors were typically the same as those in the 0–20 cm surface layer (Figure 3).

In the 0–20 cm soil layer, the VIP scores of silt and sand were much higher than 1, which had a good prediction for all aggregate stability indexes ( $R_{0.25}$ , GMD, MWD) (Figure 5). In the 20–40 cm soil layer, except for silt and sand, clay content, SOC, and root biomass can predict soil aggregate indexes well, with VIP scores almost higher than 1 (Figure 5).



(a) 0–20 cm



(b) 0–20 cm

**Figure 3.** Heat map of the correlation matrix of the independent variables used in the PLSR analysis. Note: 0.25–2 indicates aggregate fraction (%) within 0.25–2 mm; 0.053–0.25 indicates microaggregate fraction (%) within 0.053–0.25 mm; <0.053 indicates silt + clay fraction; MWD indicates mean weight diameter; GMD indicates mean geometric diameter; R<sub>0.25</sub> indicates macroaggregate fraction with diameter >0.25 mm; SOC indicates soil organic carbon; Macro-SOC indicates macroaggregate-associated SOC; Micro-SOC indicates microaggregate-associated SOC; Silt + clay-SOC indicates SOC within silt + clay fraction; EE-GRSP and T-GRSP indicate easily extractable and total glomalin-related soil protein; \* indicates a significant correlation between the two variables ( $p < 0.05$ ) and RDMD indicates root dry weight density.

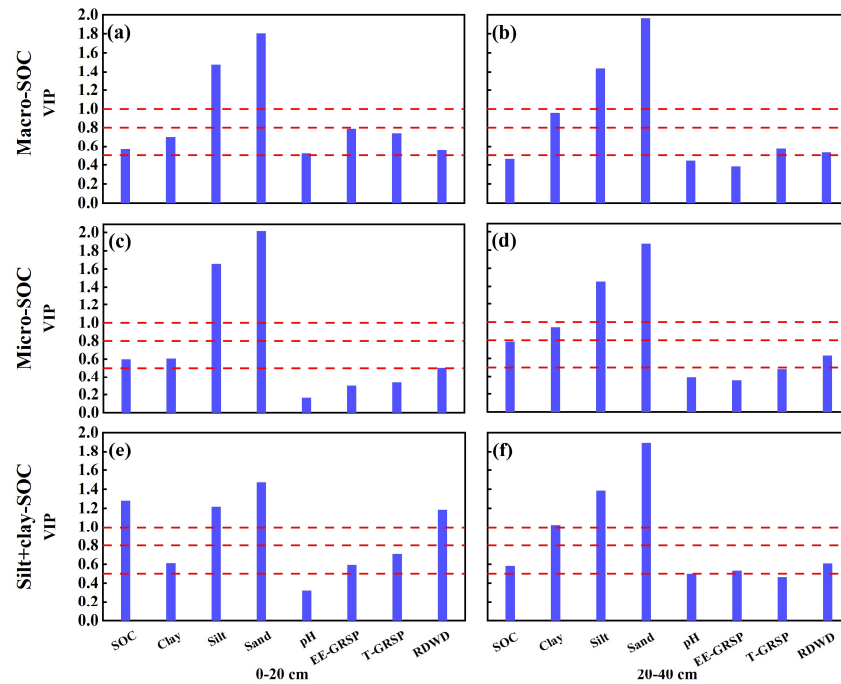


**Figure 4.** Variable importance values for the projection affecting soil aggregate-associated SOC. Note: SOC indicates soil organic carbon; Macro-SOC indicates macroaggregate-associated SOC; Micro-SOC indicates microaggregate-associated SOC; Silt + clay-SOC indicates SOC within silt + clay fraction; clay, silt and sand indicates clay, silt and sand content; EE-GRSP and T-GRSP indicate easily extractable and total glomalin-related soil protein; and RDMD indicates root dry weight density. According to the legend, (a,c,e) and e represent 0–20 cm soil lay; (b,d,f) represent 20–40 cm soil layer, respectively.

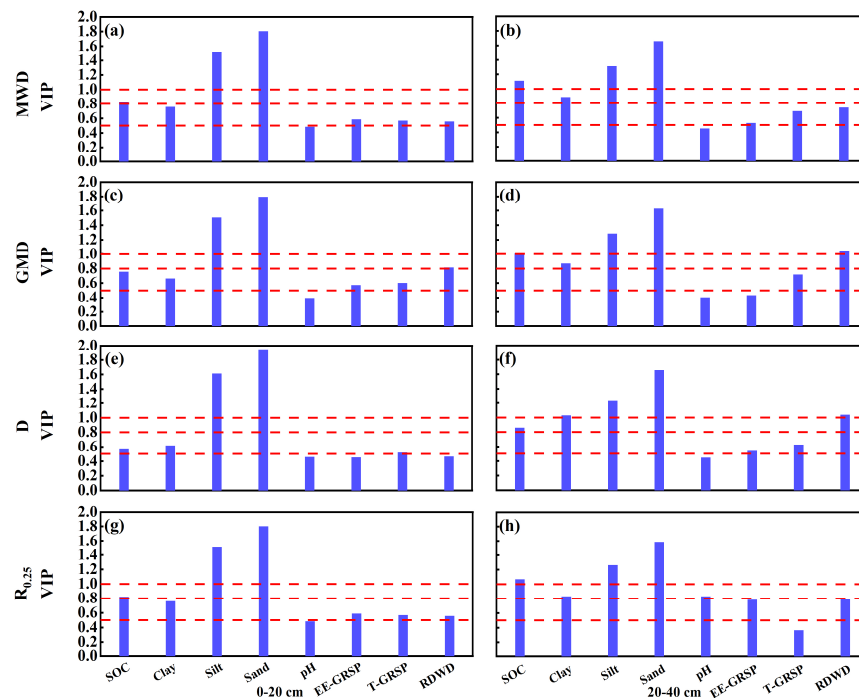


**Figure 5.** Variable importance values for the projection affecting soil aggregate stability indexes. Note: MWD indicates mean weight diameter; GMD indicates mean geometric diameter;  $R_{0.25}$  indicates macroaggregate fraction with diameter > 0.25 mm; D indicates fractal dimension; SOC indicates soil organic carbon; clay, silt and sand indicates clay, silt and sand content; EE-GRSP and T-GRSP indicate easily extractable and total glomalin-related soil protein; and RDMD indicates root dry weight density. According to the legend, (a,c,e,g) represent 0–20 cm soil lay; (b,d,f,h) represent 20–40 cm soil layer, respectively.

## 4. Discussion

### 4.1. Response of Soil Aggregate Stability and Aggregate-Associated SOC to Land Use Conversion

With the conversion of grassland to cropland, MWD, GMD and  $R_{0.25}$  decreased significantly (Figure 2,  $p < 0.05$ ). This result was consistent with Baranian Kabir et al. (2017) [31]. A possible explanation for this might be that grassland had more input of plant residues, thus improving microbial activity, promoting the formation of cementing materials, and enhancing the stability of soil aggregates [32,33]. Another possible explanation for this was that large numbers of plant roots in grassland can promote the formation and stability of aggregates through root entanglement or the cementation of root exudates [34]. On the contrary, tillage measures in cropland would break up macroaggregates in soil, resulting in a decline in the stability of soil aggregates [35].

SOC reduced significantly after grassland was converted into cropland (Table 4,  $p < 0.01$ ). This also accorded with earlier observations by Qiu et al. (2012), which showed that the conversion of grassland to cropland would result in SOC loss of more than 50% [36]. The observed decline in SOC could be attributed to the destruction of soil structure by the reclamation of grassland for cropland, which modified soil temperature, moisture and permeability, accelerated the decomposition of SOC, and ultimately led to a large loss of SOC [37]. From the perspective of the aggregate fraction, with the transformation of grassland into cropland, the increase in microaggregate percentage and the significant reduction of microaggregate-associated SOC accounted for the loss of SOC (Table 2, Table 4,  $p < 0.05$ ). As cropland was abandoned, the decrease in SOC within macroaggregate and silt + clay fractions could, in part, explain the distinct SOC loss (Table 4,  $p < 0.05$ ).

### 4.2. Factors Controlling Aggregate-Associated SOC

As depicted in Figure 3, there was a significant positive correlation between SOC within the silt + clay fraction and silt content ( $p < 0.05$ ). The observed correlation was due to the fact that, as relatively fine particles in soil, silt particles easily formed macroaggregates with root secretions and mycelia, which was conducive to the accumulation of SOC in the silt + clay fraction [38]. Moreover, silt was the soil particle type with the highest proportion in the studied region (Table 1). Significant positive correlation between glomalin-related soil protein (EE-GRSP, T-GRSP) and SOC within silt + clay fractions (Figure 3,  $p < 0.05$ ) was observed. This happened because glomalin-related soil protein was known as the “super glue” [39], which could bind silt particles to form SOC within the silt + clay fraction in this study. Together, these results provided important insights into the formation mechanism of SOC within the silt + clay fraction in this study, which was the combination of silt particles and glomalin-related soil protein.

With regard to microaggregate-associated SOC, the most interesting result to emerge was that, like SOC within the silt + clay fraction, microaggregate-associated SOC was significantly positively correlated with silt content and glomalin-related soil protein (EE-GRSP, T-GRSP), and had a good positive correlation with SOC within the silt + clay fraction (Figure 3,  $p < 0.05$ ). Therefore, it can be inferred that the binding of silt particles with glomalin-related soil protein was the main mechanism of the formation of both SOC within silt + clay and microaggregate fractions. However, there was no significant relationship between macroaggregate-associated SOC and silt content, or glomalin-related soil protein (EE-GRSP, T-GRSP) ( $p > 0.05$ ). This could be ascribed to the fact that the formation mechanism of macroaggregate-associated SOC was more complex [40], resulting in the insignificant effects of silt content and glomalin-related soil protein on SOC in the macroaggregate.

Through the analysis of PLR and VIP, the SOC in each soil layer and aggregate fraction could be predicted well by silt and sand particles (Figure 4, VIP values  $> 1$ ). The reason might be that the weak microbial activity in the high-altitude area [12] led to the universally and significantly higher contribution rate of abiotic factors (represented by silt particles) to SOC within aggregate fractions than that of biological factors (represented by RDWD EE-GRSP, T-GRSP).

#### 4.3. Factors Controlling Soil Aggregate Stability

MWD, GMD and  $R_{0.25}$ , which represented the stability of aggregates, were significantly positively correlated with SOC (Figure 3,  $p < 0.05$ ). This finding was in agreement with a previous study by Zhu et al. (2018) [41]. This could be due to the fact that SOC was the concentrated embodiment of organic cementing material in aggregates, which could effectively increase the proportion of the macroaggregate and improve the stability of aggregates [2]. Significant positive associations (Figure 3,  $p < 0.05$ ) were detected between soil aggregate stability indexes ( $R_{0.25}$ , MWD, GMD) and glomalin-related soil proteins (EE-GRSP, T-GRSP). The study of Zhang et al. and Spohn et al. also reached a consistent result [42,43]. As the secretions of rhizocorrhiza arbuscular fungi, glomalin-related soil proteins acted as the main soil organic cementing agents [39], the content of which was closely related to the stability of aggregates [44].

As can be seen from Figure 3, SOC was significantly positively correlated with aggregate stability indexes ( $p < 0.05$ ). However, no significant relationship between macroaggregate-associated SOC and aggregate stability indexes existed ( $p > 0.05$ ); only SOC in microaggregate and silty + clay fractions were significantly positively correlated with the stability indexes of aggregates ( $p < 0.05$ ). This finding indicated that the primary SOC contributor to the stability of aggregates were the SOC within microaggregates and silt + clay fractions. Regarding soil particles, aggregate stability indexes were significantly positively correlated with silt, and negatively regulated by sand (Figure 3). The same results were also found in the study by Caravaca et al. (2001), who suggested that small particles such as silt could easily bind to soil organic cementing substances (i.e., glomalin-related soil protein) to promote the formation of aggregates [38].

According to Figure 5, it could be seen that silt and sand particles, representing abiotic factors, had the best predictive ability for aggregate stability, followed by SOC and root biomass, representing biological factors. This indicated that in the high-altitude area where plant growth and microbial activity were weak, the influence of abiotic factors on the stability of soil aggregates was obviously greater than that of biological factors.

#### 5. Conclusions

To clarify the changes and driving mechanisms of soil aggregate structure, organic carbon, and their relationships during land use change in the eastern Qinghai–Tibet Plateau, soil samples of 0–20, 20–40 cm soil layers in cropland, grassland and abandoned land were collected and determined. Conclusions are as follows:

- (1) Soil aggregate stability decreased significantly with the conversion from grassland to cropland ( $p < 0.05$ ); the aggregate stability of abandoned land was slightly higher than that of cropland ( $p > 0.05$ ); the aggregate stability of grassland was significantly higher than that of abandoned land ( $p < 0.05$ );
- (2) As grassland was converted to cropland, soil organic carbon (SOC) reduced remarkably ( $p < 0.05$ ), which was because microaggregates and microaggregate-associated SOC increased significantly synchronously during this process ( $p < 0.05$ );
- (3) Soil aggregate stability was significantly positively correlated with SOC, microaggregate-associated SOC and SOC within silt + clay fraction ( $p < 0.05$ ); significant positive associations were also detected between soil aggregate stability and silt content, and glomalin-related soil protein ( $p < 0.05$ );
- (4) There was a significant positive correlation between SOC in bulk soil, and silt + clay and microaggregate fractions, which were all positively correlated with silt particles and glomalin-related soil protein ( $p < 0.05$ ), suggesting that the combination of fine physical particles (represented by silt particles) and organic cementing material (represented by glomalin-related soil protein) may be the main mechanism of SOC formation in the studied region;

- (5) Based on partial least squares regression, silt and sand could well predict aggregate stability and aggregate-associated SOC, followed by bulk organic carbon and glomalin-related soil protein, indicating that, compared with biotic factors, abiotic factors represented by silt and sand were more effective in predicting aggregate stability and aggregate-associated SOC.

**Author Contributions:** Conceptualization, Y.Z.; Methodology, Y.Z.; Software, Y.L.; Validation, R.L.; Formal analysis, Y.Z.; Investigation, Y.L., Z.C., Z.M. and H.S.; Resources, Y.Z. and R.L.; data curation, Y.L.; Writing—original draft preparation, Y.Z.; Writing—review and editing, Y.Z.; Visualization, Y.L.; Supervision, R.L. and Y.Z.; Project administration, Y.Z. and R.L.; Funding acquisition, Y.Z. All authors have read and agreed to the published version of the manuscript.

**Funding:** This research was funded by National Natural Science Foundation of China (grant number U20A20115,42207375) and the Natural Science Foundation of Qinghai Province, China (grant number 2020-ZJ-967Q).

**Institutional Review Board Statement:** Not applicable.

**Informed Consent Statement:** Not applicable.

**Data Availability Statement:** The data are available from the corresponding author on reasonable request.

**Acknowledgments:** The authors are grateful to the editor and reviewers for their valuable comments and suggestions.

**Conflicts of Interest:** The authors declare no conflicts of interest.

## References

- Rounsevell, M.D.A.; Evans, S.P.; Bullock, P. Climate change and agricultural soils: Impacts and adaptation. *Clim. Change* **1999**, *43*, 683–709. [[CrossRef](#)]
- Oades, J.M.; Waters, A.G. Aggregate hierarchy in soils. *Soil Res.* **1991**, *29*, 815–828. [[CrossRef](#)]
- Seybold, C.A.; Herrick, J.E. Aggregate stability kit for soil quality assessments. *Catena* **2001**, *44*, 37–45. [[CrossRef](#)]
- Abdalla, M.; Hastings, A.; Chadwick, D.R.; Jones, D.L.; Evans, C.D.; Jones, M.B.; Rees, R.; Smith, P. Critical review of the impacts of grazing intensity on soil organic carbon storage and other soil quality indicators in extensively managed grasslands. *Agric. Ecosyst. Environ.* **2018**, *253*, 62–81. [[CrossRef](#)]
- Mao, Z.; Li, Q.; Wang, Y. Research on the application of a cement and soil aggregate for the ecological restoration of vegetation in artificial soil. *PeerJ* **2023**, *11*, e14657. [[CrossRef](#)]
- Blankinship, J.C.; Fonte, S.J.; Six, J.; Schimel, J.P. Plant versus microbial controls on soil aggregate stability in a seasonally dry ecosystem. *Geoderma* **2016**, *272*, 39–50. [[CrossRef](#)]
- Lützw, M.V.; Kögel-Knabner, I.; Ekschmitt, K.; Matzner, E.; Guggenberger, G.; Marschner, B.; Flessa, H. Stabilization of organic matter in temperate soils: Mechanisms and their relevance under different soil conditions—A review. *Eur. J. Soil Sci.* **2006**, *57*, 426–445. [[CrossRef](#)]
- Abid, M.; Lal, R. Tillage and drainage impact on soil quality: I. Aggregate stability, carbon and nitrogen pools. *Soil Till. Res.* **2008**, *100*, 89–98. [[CrossRef](#)]
- Foley, J.A.; DeFries, R.; Asner, G.P.; Barford, C.; Bonan, G.; Carpenter, S.R.; Chapin, F.; Coe, M.; Daily, G.; Gibbs, H.; et al. Global consequences of land use. *Science* **2005**, *309*, 570–574. [[CrossRef](#)]
- Bartholome, E.; Belward, A.S. GLC2000: A new approach to global land cover mapping from Earth observation data. *Remote Sens. Environ.* **2005**, *26*, 1959–1977. [[CrossRef](#)]
- Kunlanit, B.; Butnan, S.; Vityakon, P. Land-use changes influencing C sequestration and quality in topsoil and subsoil. *Agronomy* **2019**, *9*, 520. [[CrossRef](#)]
- Sun, Z.; Duan, S.; Jiang, Y.; Wang, Q.; Zhang, G. Dominant aggregate binding agent dynamics of quaternary ancient red soils under different land use patterns. *Agronomy* **2023**, *13*, 1572. [[CrossRef](#)]
- Parton, W.J.; Scurlock, J.M.O.; Ojima, D.S.; Schimel, D.S.; Hall, D.O.; Scopegram Group Members. Impact of climate change on grassland production and soil carbon worldwide. *Glob. Chang. Biol.* **1995**, *1*, 13–22. [[CrossRef](#)]
- Wang, Z.; Ma, S.; Hu, Y.; Chen, Y.; Jiang, H.; Duan, B.; Lu, X. Links between chemical composition of soil organic matter and soil enzyme activity in alpine grassland ecosystems of the Tibetan Plateau. *Catena* **2022**, *218*, 106565. [[CrossRef](#)]
- Dong, S.; Zhang, J.; Li, Y.; Liu, S.; Dong, Q.; Zhou, H.; Yeomans, J.; Li, Y.; Li, S.; Gao, X. Effect of grassland degradation on aggregate-associated soil organic carbon of alpine grassland ecosystems in the Qinghai-Tibetan Plateau. *Eur. J. Soil Sci.* **2020**, *71*, 69–79. [[CrossRef](#)]

16. Ma, L.; Wang, Q.; Shen, S. Response of soil aggregate stability and distribution of organic carbon to alpine grassland degradation in Northwest Sichuan. *Geoderma Reg.* **2020**, *22*, e00309.
17. Pu, Y.; Lang, S.; Wang, A.; Zhang, S.; Li, T.; Qian, H.; Wang, G.; Jia, Y.; Xu, X.; Yuan, D.; et al. Distribution and functional groups of soil aggregate-associated organic carbon along a marsh degradation gradient on the Zoige Plateau, China. *Catena* **2022**, *209*, 105811. [[CrossRef](#)]
18. Li, Y.; Ma, Z.; Liu, Y.; Cui, Z.; Mo, Q.; Zhang, C.; Sheng, H.; Wang, W.; Zhang, Y. Variation in soil aggregate stability due to land use changes from alpine grassland in a high-altitude watershed. *Land* **2023**, *12*, 393. [[CrossRef](#)]
19. Guo, Z.B.; Yan, G.; Zhang, R.H.; Li, F.M.; Zeng, Z.X.; Liu, H. Improvement of soil physical properties and aggregate-associated C, N, and P after cropland was converted to grassland in semiarid loess plateau. *Soil Sci.* **2010**, *175*, 99–104. [[CrossRef](#)]
20. Kocyyigit, R.; Demirci, S. Long-term changes of aggregate-associated and labile soil organic carbon and nitrogen after conversion from forest to grassland and cropland in northern Turkey. *Land Degrad. Dev.* **2012**, *23*, 475–482. [[CrossRef](#)]
21. Zhu, G.Y.; Shangguan, Z.P.; Deng, L. Variations in soil aggregate stability due to land use changes from agricultural land on the Loess Plateau, China. *Catena* **2021**, *200*, 105181. [[CrossRef](#)]
22. Zhang, L.; Tan, X.; Chen, H.; Liu, Y.; Cui, Z. Effects of Agriculture and Animal Husbandry on Heavy Metal Contamination in the Aquatic Environment and Human Health in Huangshui River Basin. *Water* **2022**, *14*, 549. [[CrossRef](#)]
23. Paudel, B.; Wu, X.; Zhang, Y.; Rai, R.; Liu, L.; Zhang, B.; Khanal, N.; Koirala, H.; Nepal, P. Farmland abandonment and its determinants in the different ecological villages of the Koshi river basin, central Himalayas: Synergy of high-resolution remote sensing and social surveys. *Environ. Res.* **2020**, *188*, 109711. [[CrossRef](#)]
24. Chen, Q.; Yang, L.; Luo, J.; Liu, F.; Zhang, Y.; Zhou, Q.; Guo, R.; Gu, X. The 300-year cropland changes reflecting climate impacts and social resilience at the Yellow River-Huangshui River Valley, China. *Environ. Res. Lett.* **2021**, *16*, 065006. [[CrossRef](#)]
25. Yu, Y.; Wei, W.; Chen, L.D.; Jia, F.Y.; Yang, L.; Zhang, H.D.; Feng, T.J. Responses of vertical soil moisture to rainfall pulses and land uses in a typical loess hilly area, China. *Solid Earth* **2015**, *6*, 595–608. [[CrossRef](#)]
26. Wei, X.; Shao, M.; Gale, W.J.; Zhang, X.; Li, L. Dynamics of aggregate-associated organic carbon following conversion of forest to cropland. *Soil Biol. Biochem.* **2013**, *57*, 876–883. [[CrossRef](#)]
27. Nelson, D.W.; Sommers, L.E. Total carbon, organic carbon, and organic matter. In *Methods of Soil Analysis, Part 2*, 2nd ed.; Page, A.L., Ed.; John Wiley & Sons: Madison, WI, USA, 1996; Volume 14, pp. 961–1010.
28. Wright, S.F.; Upadhyaya, A. Extraction of an abundant and unusual protein from soil and comparison with hyphal protein of arbuscular mycorrhizal fungi. *Soil Sci.* **1996**, *161*, 575–586. [[CrossRef](#)]
29. Liu, H.; Zhang, M.; Lin, Z. Relative importance of climate changes at different time scales on net primary productivity—A case study of the Karst area of northwest Guangxi, China. *Environ. Monit. Assess.* **2017**, *189*, 1–11. [[CrossRef](#)]
30. Hoover, A.N.; Emerson, R.; Cortez, M.; Owens, V.; Wolfrum, E.; Payne, C.; Crawford, J.F.; Farris, R.C.; Heaton, J.H.; Mayton, S.K.; et al. Key environmental and production factors for understanding variation in switchgrass chemical attributes. *GCB Bioenergy* **2022**, *14*, 776–792. [[CrossRef](#)]
31. Baranian Kabir, E.; Bashari, H.; Mosaddeghi, M.R.; Bassiri, M. Soil aggregate stability and organic matter as affected by land use change in central Iran. *Arch. Agron. Soil Sci.* **2017**, *63*, 615–631. [[CrossRef](#)]
32. Zhao, F.Z.; Fan, X.D.; Ren, C.J.; Zhang, L.; Han, X.H.; Yang, G.H.; Wang, J.; Doughty, R. Changes of the organic carbon content and stability of soil aggregates affected by soil bacterial community after afforestation. *Catena* **2018**, *171*, 622–631. [[CrossRef](#)]
33. Ayoubi, S.; Karchegani, P.M.; Mosaddeghi, M.R.; Honarjoo, N. Soil aggregation and organic carbon as affected by topography and land use change in western Iran. *Soil Till. Res.* **2012**, *121*, 18–26. [[CrossRef](#)]
34. Poirier, V.; Roumet, C.; Munson, A.D. The root of the matter: Linking root traits and soil organic matter stabilization processes. *Soil Biol. Biochem.* **2018**, *120*, 246–259. [[CrossRef](#)]
35. Six, J.A.E.T.; Elliott, E.T.; Paustian, K. Soil macroaggregate turnover and microaggregate formation: A mechanism for C sequestration under no-tillage agriculture. *Soil Biol. Biochem.* **2000**, *32*, 2099–2103. [[CrossRef](#)]
36. Qiu, L.; Wei, X.; Zhang, X.; Cheng, J.; Gale, W.; Guo, C.; Long, T. Soil organic carbon losses due to land use change in a semiarid grassland. *Plant Soil* **2012**, *355*, 299–309. [[CrossRef](#)]
37. Li, G.L.; Pang, X.M. Effect of land-use conversion on C and N distribution in aggregate fractions of soils in the southern Loess Plateau, China. *Land Use Pol.* **2010**, *27*, 706–712. [[CrossRef](#)]
38. Caravaca, F.; Lax, A.; Albaladejo, J. Soil aggregate stability and organic matter in clay and fine silt fractions in urban refuse-amended semiarid soils. *Soil Sci. Soc. Am. J.* **2001**, *65*, 1235–1238. [[CrossRef](#)]
39. Cross, T.A. Global Distributions of Arbuscular Mycorrhizal Fungi. *Ecosystems* **2006**, *9*, 305–316.
40. Wang, J.; Shu, K.; Wang, S.; Zhang, C.; Feng, Y.; Gao, M.; Cai, H. Soil enzyme activities affect SOC and TN in aggregate fractions in sodic-alkali soils, Northeast of China. *Agronomy* **2022**, *12*, 2549. [[CrossRef](#)]
41. Zhu, G.; Deng, L.; Shangguan, Z. Effects of soil aggregate stability on soil N following land use changes under erodible environment. *Agric. Ecosyst. Environ.* **2018**, *262*, 18–28. [[CrossRef](#)]
42. Zhang, S.; Li, Q.; Zhang, X.; Wei, K.; Chen, L.; Liang, W. Effects of conservation tillage on soil aggregation and aggregate binding agents in black soil of Northeast China. *Soil Till. Res.* **2012**, *124*, 196–202. [[CrossRef](#)]

43. Spohn, M.; Giani, L. Water-stable aggregates, glomalin-related soil protein, and carbohydrates in a chronosequence of sandy hydromorphic soils. *Soil Biol. Biochem.* **2010**, *42*, 1505–1511. [[CrossRef](#)]
44. Wright, S.F.; Upadhyaya, A. A survey of soils for aggregate stability and glomalin, a glycoprotein produced by hyphae of arbuscular mycorrhizal fungi. *Plant Soil* **1998**, *198*, 97–107. [[CrossRef](#)]

**Disclaimer/Publisher’s Note:** The statements, opinions and data contained in all publications are solely those of the individual author(s) and contributor(s) and not of MDPI and/or the editor(s). MDPI and/or the editor(s) disclaim responsibility for any injury to people or property resulting from any ideas, methods, instructions or products referred to in the content.